

# MAGNETIC FIELD AND FORCE CALCULATION OF THE NEW SCU PROTOTYPES\*

Y. Shiroyanagi<sup>†</sup>, E. Anliker, M. Kasa, I. Kesgin, Y. Ivanyushenkov  
Argonne National Laboratory, Lemont, IL, USA

## Abstract

New 0.5-m-long superconducting undulator (SCU) magnet prototypes were designed based on lessons learned from the previous full-length (1.5-m) magnet experiences. The original monolithic magnets have all-steel poles. The new cores have plastic-back poles to avoid electrical shorts of superconducting wires to cores. A magnetostatic calculation was made for a one-period model for each of two designs under consideration. Then magnetostatic and mechanical analyses were also conducted for the prototype SCUs with period lengths of 29.5 mm and 23.5 mm. The software used for this simulation is ANSYS Maxwell and Mechanical. Both the magnetostatic and the mechanical analyses confirm the validity of the new design.

## INTRODUCTION

New prototypes of superconducting undulators (SCUs), measuring 0.5 meters in length, have been developed by incorporating lessons learned from earlier designs of full-length (1.5-meter) magnets. These prototypes utilize a 0.6-mm-diameter Nb-Ti wire as the conductor. Unlike the original monolithic magnets, which featured all-steel poles, the updated designs integrate plastic-back poles to prevent electrical shorts between the superconducting wires and the cores. The detailed design of these prototypes, including the use of plastic poles, has been finalized [1]. This paper compares the magnetostatic calculations and mechanical analyses of the original and new prototypes, which feature 29.5 and 23.5 periods, respectively. Electromagnetic simulations were performed using ANSYS Maxwell, while structural analyses were conducted using ANSYS Mechanical [2]. A summary of the SCU parameters is presented in Table 1. Additionally, the end correction scheme has been implemented and is explained in a later section [3].

Table 1: SCU Parameters

	Unit	Value
Period Length	mm	16.5
Periods	N	23.5 or 29.5
Magnetic Gap	mm	8
Pole Width	mm	3
Groove Width	mm	5.25
Groove Depth	mm	4.15
Full Coil Turns	N	53
Conductor Dia.	mm	0.6
Main Current	A	450

\* Work supported by the U.S. DOE Office of Science-Basic Energy Sciences, under Contract No. DE-AC02-06CH11357.

<sup>†</sup> email address: yshiroyanagi@anl.gov

## ONE-PERIOD MODEL

Magnetic fields and forces were calculated using a one-period model with periodic boundary conditions for three different configurations: an air core (without steel), a full-steel pole design, and a new design incorporating both plastic and steel poles.

### Air Core

The magnetic field was calculated for the coils-only case (air core) using periodic boundary condition in the z-direction,  $\mathbf{B}(z + z_0) = \mathbf{B}(z)$ ,  $z_0 = 16.5$  mm. Figure 1(a) illustrates the geometry of the four coils and the direction of the currents. The maximum field on the axis  $B_{\text{peak}}$  is 0.669 T at 450 A as shown in Fig. 1(b). The magnetic field within the conductor is depicted in the cross section in Fig. 1(c), while the overall field distribution is shown in Fig. 1(d). The maximum field,  $B_{\text{max}} = 2.20$  T, occurs at the edge of the conductor. Figure 1(e) shows the forces acting on one coil ( $F_x, F_y$ ) at six coil segments. The force at each section of the conductor is directed outward, as indicated.

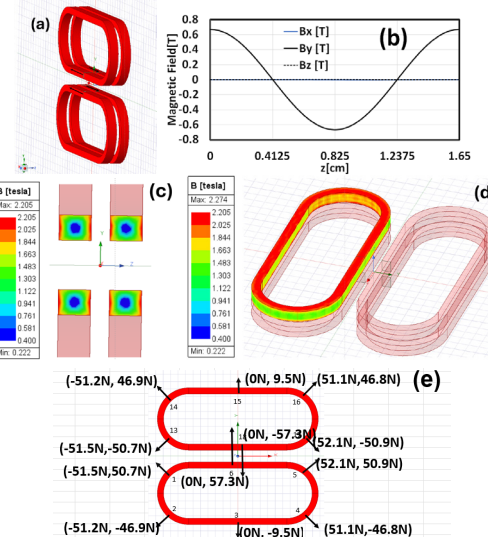


Figure 1: (a) Geometry, (b) on-axis magnetic field, (c) magnetic field at y-z cross-section of the coils, (d) magnetic field in one of the coils, (e) magnetic forces on a top coil and a bottom coil in six segments.

The total force on the top coils is  $F_y = -111.5$  N, while the total force on the bottom coils is  $F_y = 111.3$  N, indicating that the forces are attractive.

## Full Steel Pole

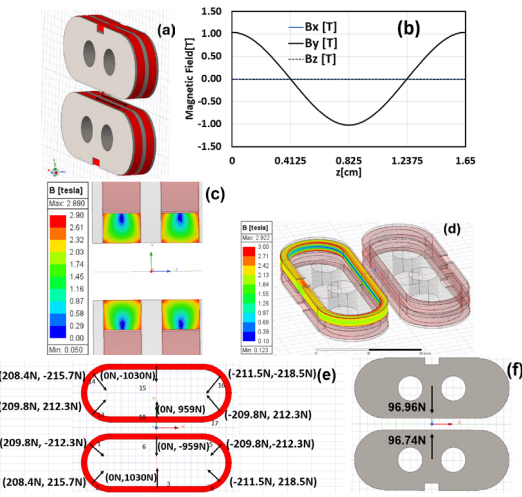


Figure 2: (a) Geometry, (b) on-axis magnetic field, (c) magnetic field in conductor at y-z cross section, (d) magnetic field in one of the coils, (e) magnetic forces on a top coil and a bottom coil in six segments, (f) magnetic forces on the core.

The magnetic field was calculated for the full-steel pole cores, corresponding to the previous magnet design. Figure 2(b) displays the on-axis magnetic field, with a peak field of  $B_{\text{peak}} = 1.03\text{T}$  at a current of 450 A. The magnetic field within the conductor is depicted in the cross section in Fig. 2(c), while the overall field distribution is shown in Fig. 2(d). The maximum field within the conductor occurs at the corner facing the groove, with  $B_{\text{max}} = 2.89\text{T}$ . The forces ( $F_x, F_y$ ) acting on each section of the coils are directed inward, toward the steel groove, as illustrated in Fig. 2(e). The forces on the cores,  $F_y=96.7\text{N}$ , attractive are depicted in Fig. 2(f). The total force on the half magnet structure, including both the coils and cores, is  $F_y=266.5\text{ N}$ , indicating an attractive force.

## Steel-Plastic Pole Core

Table 2: Summary of One-Period Model

	Coil only	Full Steel	Steel-Plastic Pole
On-axis field [T]	0.669	1.031	1.03
Maximum field in conductor [T]	2.20	2.89	2.87
Force per period [N]	111.3	266.5	218.7

Figure 3(a) illustrates the model geometry of the new core design. The backside poles are constructed from plastic (Ultem), while the model incorporates a square cross-section component made of 1018 steel. Figure 3(b) displays the on-axis magnetic field, with a peak field of  $B_{\text{peak}} = 1.03\text{T}$  at a current of 450 A. The magnetic field distribution within the conductor is depicted in the cross-section view in Fig. 3(c), and the overall field distribution is presented in Fig. 3(d). The maximum magnetic field within the conductor occurs at the corner facing the groove, with  $B_{\text{max}} = 2.87\text{T}$ .

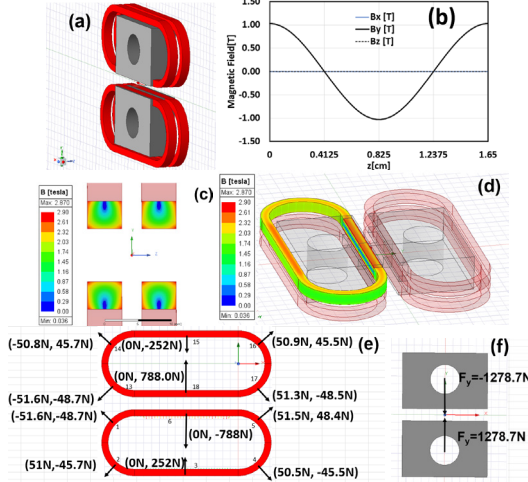


Figure 3: (a) Geometry, (b) on-axis magnetic field, (c) magnetic field in conductor at y-z cross section, (d) magnetic field in one coil, (e) magnetic forces on a top coil and a bottom coil in six segments, (f) magnetic forces on the core.

The forces ( $F_x, F_y$ ) acting on each section of the coils near the steel part are directed inward, toward the steel, while in the air section, they are directed outward, as illustrated in Fig. 3(e). The forces acting on the cores are depicted in Fig. 3(f). The total force on the half-magnet structure, including both the coils and cores, is  $F_y=218.7\text{ N}$ , indicating an attractive force. The results obtained from the one-period model are summarized in Table 2. Notably, the steel-plastic pole core produces the same on-axis magnetic field as the full-steel pole core but exhibits a reduced force per period.

## 23.5/29.5 PERIOD MODEL

### Full-Steel Pole Core

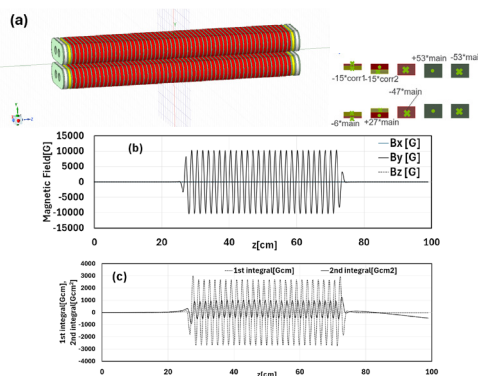


Figure 4: (a) Model geometry with the end correction, (b) calculated on-axis magnetic field, (c) 1<sup>st</sup> and 2<sup>nd</sup> integrals of the on-axis magnetic field.

The magnetic field was calculated for a model with a length of 0.5 m (29.5 periods) and a period of 16.5 mm, incorporating end corrections. Figure 4(a) illustrates the overall geometry used for the magnetostatic model and the end correction schemes. In all cases, the main current is set

to 450 A, with 53 turns per groove. At the ends, the number of main turns is reduced to 47, 27, and 6 turns in the last three grooves, respectively.

Additionally, corrector turns, with 15 turns each, are wound on the first and second grooves [2]. The correction current is optimized at 9.77 A. The on-axis peak magnetic field is  $B_{\text{peak}} = 1.03$  T, as shown in Fig. 4(b), with the first integral of  $29.7 \mu\text{Tm}$  ( $29.7 \text{ G}\cdot\text{cm}$ ) and the second integral of  $-4.71 \mu\text{Tm}^2$  ( $-471 \text{ G}\cdot\text{cm}^2$ ), as shown in Fig. 4(c). As summarized in Table 3, the total force on the coil and core per period is  $7196.2 \text{ N} / 29.5 = 243 \text{ N}$ , representing an attractive force. This value is slightly lower than the 266 N that is calculated for a one-period case, as the forces at the ends are reduced. If the end period is ignored, the force per period becomes  $7196.2 \text{ N} / 27.5 = 261.7 \text{ N}$ .

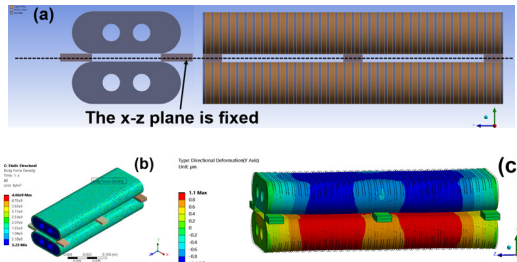


Figure 5: (a) Front and side views of the model, (b) calculated force density is transferred to mechanical model, (c) deformation of the 1006 steel core.

Figure 5(a) shows the front and side views of the model, where Nb-Ti conductor is modeled as copper, and the core is made of 1006 steel. The center horizontal plane ( $y=0$ ) is fixed, as indicated by the dotted line. The magnetic force distribution, transferred from the magnetostatic model, is illustrated in Fig. 5(b). In Fig. 5(c), the maximum deformation of the core is calculated as  $dy = 1.1 \mu\text{m}$ , resulting in a reduction of the magnetic gap by  $2.2 \mu\text{m}$ . The maximum stress, occurring at the gap spacers, is 32.3 MPa (not shown). Figure 6(a) illustrates the model geometry and the end correction scheme, which is identical to that of the full-steel pole SCU. In this model, the gap-side of the core is made of 1018 steel, while the backside is made of plastic (Ultem). The core consists of 23.5 periods, with a total length of 0.39 m. The Nb-Ti conductor is approximated as copper in the model. Since plastic components are non-magnetic, they are excluded from the magnetostatic model. The magnetic field was calculated for an operational current of 450 A, with an optimal correction current of 9.4 A. The on-axis magnetic field is shown in Fig. 6(b), where the peak field is  $B_{\text{peak}} = 1.03$  T. The first integral is  $67.7 \mu\text{Tm}$  ( $67.7 \text{ G}\cdot\text{cm}$ ), and the second integral is  $1.80 \mu\text{Tm}^2$  ( $180 \text{ G}\cdot\text{cm}^2$ ), as presented in Fig. 6(c). As summarized in Table 3, the total force is an attractive force. The force per period is calculated as  $5022 / 23.5 = 213.7 \text{ N}$ , which is slightly lower than the one period case due to reduced forces at the ends. Additionally, no difference was observed in the peak field between the footed and non-footed sections. Figure 7(a) shows the front and side views of the mechanical model. The Nb-Ti conductor is modeled as copper, and the core is made of 1018 steel.

### Steel-Plastic Pole

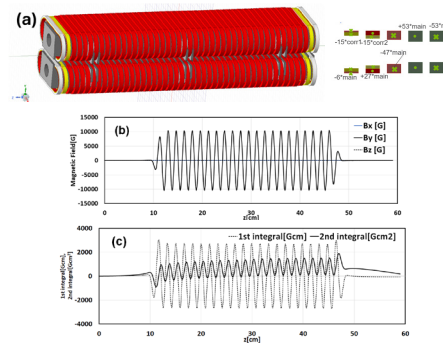


Figure 6: (a) Model geometry with the end correction, (b) calculated on-axis magnetic field, (c) 1<sup>st</sup> and 2<sup>nd</sup> integrals of the on-axis magnetic field.

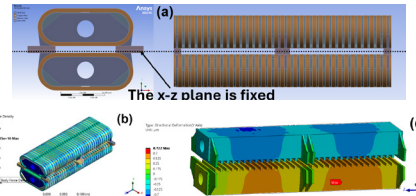


Figure 7: (a) Front and side views of the model (b) calculated force density is transferred to mechanical model, (c) deformation of the 1018 steel core.

The plastic used in this model is Ultem [1]. The center horizontal plane ( $y=0$ ) is fixed, as indicated by the dotted line. In Fig. 7(b), the calculated force density from the previous magnetic model is transferred to the mechanical model. Figure 7(c) illustrates the deformation of the 1018 steel core, which is  $0.7 \mu\text{m}$  per side, resulting in a total reduction of the magnetic gap by  $1.4 \mu\text{m}$ . The maximum stress is 33 MPa at the ends (not shown). Table 3 summarizes the comparison between the full pole core and the steel-plastic core. The force per period is lower for the steel-plastic core.

Table 3: Full Pole and Steel-Plastic Pole SCUs

	Full Steel-Pole	Steel-Plastic Pole
On-axis field [T]	1.03	1.035
Force per period [N]	243	213
Magnetic gap change [ $\mu\text{m}$ ]	2.2	1.4

### CONCLUSION

The on-axis peak magnetic field of the new steel-plastic core is identical to that of the original full-steel pole core, despite the reduced amount of steel. In both configurations, the magnetic gap decreases by approximately  $2 \mu\text{m}$  at an operating current of 450 A. The new design offers significantly improved electrical insulation without compromising magnetic or mechanical performance.

### ACKNOWLEDGEMENT

Author acknowledges J. Xu and M. Qian for useful discussion.

## REFERENCES

- [1] E. Anliker *et al.*, “The Design and Manufacturing of Superconducting Undulator Magnets Utilizing Additive Manufacturing & Plastic Components,” presented at CEC-ICMC 2025, Reno, NV, USA, May 2025.  
<https://indi.to/3TRLB>
- [2] ANSYS Mechanical, <https://www.ansys.com>
- [3] Y. Shiroyanagi *et al.*, “Magnetic Field Calculation of Superconducting Undulators for FEL Using Maxwell 3D,” in *Proc. NAPAC2022*, Albuquerque, NM, USA, Aug. 2022, pp. 423-426.  
[doi:10.18429/JACoW-NAPAC2022-TUPA33](https://doi.org/10.18429/JACoW-NAPAC2022-TUPA33)